Shielding and Transportability Assessment for Determining the Maximum Thermal Power of a Mobile HTGR

Woo Seok Choi, Jeong Ik Lee
⁎ Dept. Nuclear & Quantum Eng., KAIST, 373-1, Guseong-dong, Yuseong-gu, Daejeon, 305-701, Republic of Korea
** Corresponding author: jeongiklee@kaist.ac.kr*

***Keywords : Mobile Microreactor, HTGR, Radiation Shielding, Transportability, OpenMC**

1. Introduction

Mobile microreactors offer a potential option for rapidly supplying power to remote and off-grid locations. Their compact configurations facilitate transport, while long refueling intervals and modular designs support rapid on-site deployment. HTGR concepts employ TRISO fuel and gas cooling, which provide high-temperature tolerance and favorable passive-safety characteristics. Project Pele is a notable transport-oriented microreactor program in which reactor modules are containerized, transported, deployed, and removed within operationally relevant timeframes [1].

For such systems, the achievable thermal power is constrained not only by reactor design but also by the coupled effects of radiation shielding and transportation. The shutdown source strength is typically proportional to the reactor thermal power if the fuel burn-up is kept constant. The shielding required to satisfy transport dose limits then increases the package envelope, module mass, and center of gravity. Consequently, a design that meets all radiological criteria may still prove impractical due to size constraints, weight restrictions, or road transport limits.

Previous studies have primarily examined shielding materials, transport dose, or occupational exposure for fixed reactor configurations [2-5]. They do not directly determine the largest reactor output that simultaneously satisfies dose, geometry, mass, and vehicle-loading constraints. This study develops an integrated framework for determining the maximum transportable thermal power of a mobile HTGR by coupling power-dependent core scaling, OpenMC-based shielding response, and CAD-based transportability analysis. The present paper demonstrates the framework using Pb as the baseline shielding material, while other candidate materials will be evaluated in future work.

2. Methodology

2.1 Scalable HTGR Module Definition and Power Scaling

The reference geometry and photon source term were derived from publicly available microreactor analyses [6,7], while the adopted container and transport constraints follow [8-10]. The parameters are summarized in Table I. The photon source energy distribution was represented using the reported 18-group decay-photon spectrum at 72 h after shutdown [7]. The spectrum is normalized per MTiHM, and the absolute groupwise source strengths were obtained using a reference heavy-metal inventory of 0.809 MTiHM. The corresponding source data are shown in Fig 1. The reference core geometry, 72 h cooling time, and photon source term were adopted from the Holos analysis [7]. The 20 ft CONEX dimensions and maximum gross mass follow ISO 668 [8], while the transport dose-rate limits follow NUREG-2216 and 10 CFR 71.47 [9,10].

Table I. Reference HTGR geometry and adopted transport constraints

Parameter	Adopted value
Reference thermal power	22 MWth
Reference active-core geometry	r_{ref}=104.54 cm, H_{ref}=300 cm
Transport cooling time	72 h
20 ft CONEX external dimensions	6.058× 2.438 × 2.591 m
Maximum package gross mass	30.48 t
Surface dose-rate limit	200 mrem/h
Dose-rate limit at 2 m	10 mrem/h

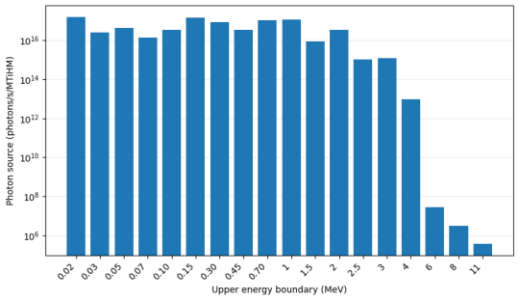


Fig. 1. 72h decay-photon spectrum per MTiHM [7]

Power scaling assumes the same HTGR fuel form, constant average power density, constant heavy-metal loading per unit active-core volume, unchanged material composition, constant discharge burnup represented by the same irradiation-history surrogate, and the same 72 h cooling time. Geometric similarity of the active core is maintained by preserving the reference height-to-diameter ratio. Defining the common linear scale factor as $s(P) = (P/P_{ref})^{1/3}$, both the core radius and active-core height scale with the cube root of thermal power, whereas the heavy-metal inventory remains proportional to power.

$$r_c(P) = r_{c,ref}\left(\frac{P}{P_{ref}}\right)^{\frac{1}{3}}, H_c(P) = H_{c,ref}\left(\frac{P}{P_{ref}}\right)^{\frac{1}{3}}$$
$$M_{HM}(P) = \frac{M_{HM,ref}P}{P_{ref}} \quad (1)$$

Over the analyzed 1.0–5.5 MWth range, the core dimensions were obtained by scaling down the 22 MWth reference geometry. This scaling assumes that the average power density, burnup, material composition, heavy-metal loading per unit volume, and core height-to-diameter ratio remain unchanged. Therefore, the scaled geometries are used only for the present shielding and transportability assessment and do not represent validated small-core designs.

The absolute source strength $S_{\gamma,g}(P)$ for photon energy group g is obtained by multiplying the reported 72 h emission rate per MTiHM, $q_{\gamma,g}(72\ h)$, by the scaled heavy-metal inventory $M_{HM}(P)$.

$$S_{\gamma,g}(P) = q_{\gamma,g}(72\ h) M_{HM}(P) \quad (2)$$

Because reactor power changes the absolute source strength and both the radial and axial self-shielding dimensions, the OpenMC response is parameterized by the common geometry scale and shield thickness rather than by power alone.

2.2 OpenMC-Based Pb Shielding Response Evaluation

The transport calculation is performed in fixed-source photon mode using OpenMC [11]. The scaled, homogenized fuel-cartridge region emits photons isotropically according to the Holos-derived 72 h energy distribution. Surrounding regions represent the pressure boundary, inherent structure, Pb transport shield, and CONEX envelope. Photon fluence is tallied in finite air cells adjacent to the package surface and at 2 m from the vehicle side, and ICRP Publication 116 fluence-to-effective-dose coefficients are applied as the operational dose metric [12].

Consistent with the 72 h source-term treatment in previous work [7], which assumes that prompt fission neutrons diminish within seconds after shutdown and evaluates the transport dose using photons from fission and activation products, residual spontaneous-fission and (α,n) neutron sources were not separately modeled. therefore, the reported $P_{max,\ Pb}$ is interpreted as a photon-only screening estimate.

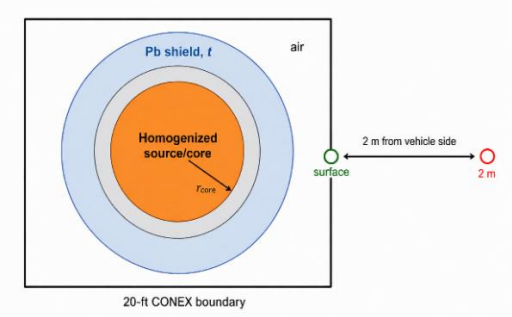


Fig. 2. OpenMC Pb transport model

The groupwise source strengths define the normalized photon-energy distribution, while the total photon source rate is given by $S_\gamma(P)=\sum_g S_{\gamma,g}(P)$. Each response point is characterized by the common geometry scale $s(P)=(P/Pref)^{1/3}$ and Pb shield thickness t. Thus, both the radial and axial source dimensions vary with thermal power. OpenMC provides the dose response per source photon, $R_k[s(P),t]$, at detector location k. In this study, k=surf and k=2m denote the surface and 2 m detectors, respectively. The physical dose rate is calculated as

$$D_k(P,t) = S_\gamma(P) R_k[s(P),t] \quad (3)$$

The Pb response database spans the adopted 1.0-5.5 MWth power range and a structured Pb thickness grid. The Holos broad-group source representations were compared with the published results for 20 and 30 cm of Pb. Among the tested representations, the lower-edge representation provided the closest agreement and was adopted for the Pb analysis. The logarithms of the dose responses were interpolated piecewise linearly in both shield thickness and geometry scale. The resulting response surface was subsequently used in the bracket-and-bisection power search.

For a trial power, Pb thickness is not treated as an independent optimization variable. Using the adopted dose-rate limits of $D_{surf,lim}$=200 mrem/h and $D_{2m,lim}$ =10 mrem/h, the required Pb thickness at trial power P is defined as

$$t_{req}(P) = min\{t \mid D_{surf}(P,t) \le D_{surf,lim}, D_{2m}(P,t) \le D_{2m,lim}\} \quad (4)$$

The resulting $t_{req}(P)$ is the minimum Pb thickness satisfying both dose-rate criteria.

2.3 CAD-Based Transportability Evaluation

Once $t_{req}(P)$ is obtained, a parameterized CAD surrogate represents the scaled reactor body, Pb shielding layer, container, skid and support frame, and tie-down and interface hardware. Reactor-body and container masses are based on public reference information, while Pb shield mass is calculated from material density and CAD volume. The skid/support and tie-down/interface masses are estimated from the parameterized CAD model and reference hardware data. A mass-growth allowance of f_m=0.20 is applied only to the preliminary support and interface mass estimates to account for unresolved design details. Defining M_{base} as the combined mass of the reactor body, Pb shield, and container, and M_{aux} as the combined mass of the support and interface components, the total module mass is calculated as

$$M_{module} = M_{base} + (1 + f_m) M_{aux}, \qquad f_m = 0.20 \quad (5)$$

The component masses and their longitudinal locations were combined to calculate the loaded-package center of gravity(x_{CG}) of the loaded package. The transported module weight W is then applied to a simplified semitrailer model, where x_K and x_B denote the longitudinal locations of the kingpin and trailer-bogie center, respectively. Static equilibrium gives the corresponding vertical reactions $R_{kingpin}$ and R_{bogie}. The kingpin reaction is subsequently distributed to the tractor steer axle and tandem drive axles using the tractor wheelbase and fifth-wheel position.

$$R_{bogie} = \frac{W(x_{CG} - x_k)}{x_B - x_k}, R_{kingpin} = W - R_{bogie} \quad (6)$$

The model adds tractor and trailer tare masses to the transported module weight to calculate the gross vehicle weight (GVW). The resulting package mass, GVW, fifth-wheel reaction, steer-axle load, drive-axle load, and trailer-axle load are then compared with the applicable limits. A configuration is feasible only when the dose criteria, CONEX envelope, package mass, road GVW, and all axle-load constraints are satisfied simultaneously.

2.4 Integrated Maximum Transportable Power Assessment

The adopted radiation criteria are 200 mrem/h at the package or vehicle side and 10 mrem/h at 2 m from the vehicle lateral surface, consistent with 10 CFR 71.47 and NUREG-2216 [9,10]. The analysis uses a 20 ft effective CONEX envelope, a 30.48 t package screening limit, a 40 t road GVW limit, a 20 t fifth-wheel rating, and a representative 6×4 tractor with a 10 t limit on each of the two drive axles, corresponding to a 20 t combined drive-tandem limit. The representative vehicle model uses a steer-axle-to-drive-tandem-center distance of 3.975 m and a steer-axle-to-fifth-wheel distance of 3.864 m. The surrogate tractor tare mass is 7.50 t, comprising 4.50 t on the steer axle and 3.00 t on the two-axle drive tandem in total.

The coupled assessment is formulated as a nested feasibility search. For each trial power P, the core geometry and source are scaled, the minimum dose-compliant Pb thickness $t_{req}(P)$ is obtained, and the resulting mass, envelope, CG, and vehicle reactions are evaluated. A coarse power scan first brackets the transition between feasible and infeasible configurations. Bisection is then applied within the bracket to determine the largest feasible power.

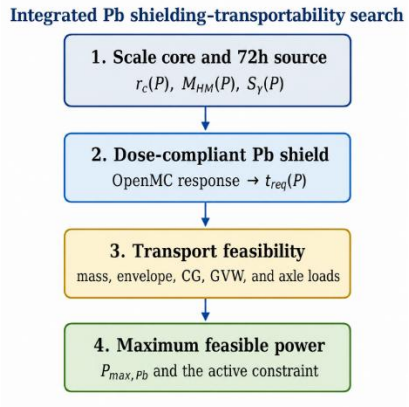


Fig. 3. Integrated search procedure for determining the maximum transportable power of the Pb-shielded module

The structured OpenMC grid is used only to construct the Pb response database. A trial configuration is assigned F(P)=1 when the dose, envelope, package-mass, GVW, fifth-wheel, and axle-load constraints are all satisfied, and F(P)=0 otherwise. The maximum transportable power of the Pb-shielded module is then defined as

$$P_{max,pb} = \max\{P: F(P) = 1\} \quad (7)$$

At $P_{max,Pb}$, one constraint, or occasionally several coincident constraints, becomes active. Identifying this active constraint shows whether further power increase requires reduced Pb mass, a larger transport envelope, a lighter module, or a different vehicle configuration.

3. Results

3.1 Pb Attenuation Benchmark

The Pb model was compared with the Holos transportation-shielding results for Pb thicknesses of 20 and 30 cm [7]. Using the selected lower-edge source representation, OpenMC predicted dose rates of 192.83 and 1.253 mrem/h, compared with 194.5 and 1.190 mrem/h, respectively, in the reference MCNP calculation. The signed relative difference was defined as $\delta_D = 100(D_{openmc}-D_{MCNP})/D_{MCNP}$, using MCNP as reference.

The resulting signed relative differences were −0.86% and +5.29% for 20 and 30 cm of Pb, respectively. The corresponding OpenMC tally relative statistical uncertainties were 4.66% and 4.95%, respectively. The OpenMC D_{30}/D_{20} dose ratio was 6.2% higher than the reference ratio, indicating that the model captures the published Pb attenuation trend over this thickness range.

Table II. Pb attenuation benchmark against the reference

Case	MCNP (mrem/h)	OpenMC (mrem/h)	OpenMC Statistical Relative Error (%)	Signed Relative Difference (%)
Pb 20 cm	194.5	192.83	4.66	-0.86
Pb 30 cm	1.190	1.253	4.95	5.29
30/20 ratio	0.006118	0.006498	-	6.21

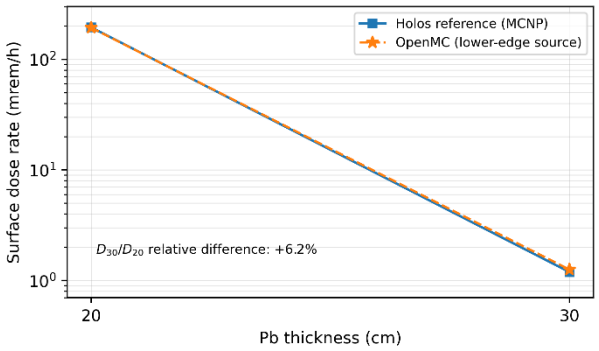


Fig. 4. OpenMC–Holos Pb attenuation benchmark

3.2 Power-Dependent Pb Shield Sizing and Transportability

The dose-compliant Pb thickness was evaluated at 1.0, 3.0, and 5.5 MWth. The corresponding core dimensions (D x H) were 74.62×107.06, 107.61×154.41, and 131.71×188.99 cm, while the required Pb thicknesses were 14.20, 15.63, and 15.73 cm. The 2 m dose criterion controlled shield sizing at all three power levels. The

thickness increased from 1.0 to 3.0 MWth and then remained nearly unchanged at 5.5 MWth, indicating that the increased source strength was partly offset by greater self-shielding in the larger core.

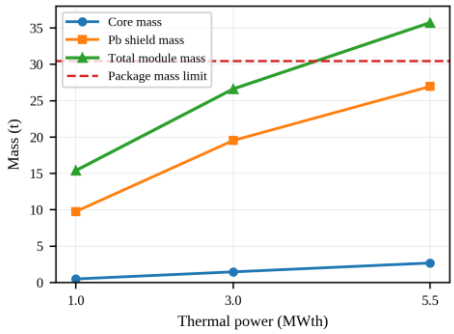


Fig. 5. Power-dependent component and module masses

As shown in Fig. 5, the core mass increased from 0.49 to 1.46 and 2.68 t, while the Pb shield mass increased from 9.76 to 19.53 and 26.97 t at 1.0, 3.0, and 5.5 MWth, respectively. The corresponding total module masses were 15.39, 26.62, and 35.74 t. Thus, although the required Pb thickness remained within a narrow range, the shield mass continued to increase because both the radial and axial dimensions of the shielded core increased with power. The 5.5 MWth module exceeded the 30.48 t package mass limit.

For the representative 6×4 tractor case, the maximum transportable power was $P_{max,Pb}$ = 2.74 MWth with t_{req} = 15.60 cm, the core and Pb shield masses were 1.34 and 18.42 t, and the total module mass and GVW were 25.33 and 38.33 t, respectively. Each of the two tractor drive axles carried 10.00 t, corresponding to a combined drive-tandem load of 20.00 t; therefore, the per-axle drive-load limit was the active constraint. The drive-axle limit was therefore reached before the package-mass, GVW, and fifth-wheel limits.

4. Conclusion and Summary

An integrated Pb shielding and transportability assessment was applied to a 20 ft CONEX HTGR module. Geometric similarity was maintained by scaling both the core radius and active-core height with the cube root of thermal power, while the heavy-metal inventory and core mass were scaled in proportion to power. The framework then determined the minimum Pb thickness satisfying the surface and 2 m dose criteria and evaluated the resulting module mass, envelope, CG, GVW, fifth-wheel reaction, and axle loads.

The OpenMC D30/D20 attenuation ratio was 6.2% higher than the Holos reference value. Over the 1.0–5.5 MWth range, the required Pb thickness increased from 14.20 to 15.73 cm, whereas the core mass increased from 0.49 to 2.68 t, the Pb shield mass from 9.76 to 26.97 t, and the total module mass from 15.39 to 35.74 t. Under the adopted vehicle model, the maximum transportable power was 2.74 MWth, with the tractor drive-axle load as the active constraint. These results show that Pb-shield mass growth is governed primarily by the increasing dimensions of the shielded core rather than by shield-thickness growth alone, and that the maximum output is determined by the coupled dose and vehicle-loading problem. The reported $P_{max,\ Pb}$ is specific to the photon-only Pb-shielding model, idealized core-scaling surrogate, and representative tractor assumptions. The reported $P_{max,Pb}$ is specific to the photon-only 72h source-term treatment, the idealized core-scaling surrogate, and the representative tractor assumptions [7]. Any residual spontaneous-fission or (α,n) contribution not represented in the Holos reference would require a separate source-term and neutron-shielding assessment. Other shielding materials will be evaluated in future work.

ACKNOWLEDGEMENTS

This work was supported by the National Research Foundation of Korea (NRF) grant funded by the Korea government (MSIT) (RS-2023-00259713).

REFERENCES

[1] U.S. Department of Defense Strategic Capabilities Office, Project Pele Mobile Microreactor Final Environmental Impact Statement, U.S. Department of Defense (2022).
[2] S. E. Bays, A. M. Ougouag, H. Hiruta, and R. H. Stewart, “Challenges and Opportunities Specific to Microreactors: Compact and Light-Weight Shielding During Operation and Transportation,” Nuclear Science and Engineering (2025).
[3] J. G. Fantidis, “The comparison between simple and advanced shielding materials for the shield of portable neutron sources,” International Journal of Radiation Research, Vol. 13, No. 4, pp. 287-296 (2015).
[4] S. J. Maheras, H. Adkins, J. Clarity, N. Kucinski, P. Stefanovic, and V. Wilson, Microreactor Incident-Free Transportation Radiation Dose Assessment, PNNL-38760, Pacific Northwest National Laboratory (2025).
[5] J. S. Choi, Study on Occupational Dose Assessment for Republic of Korea Army Micro-Reactor Operations by Shielding Design, M.S. Thesis, Korea Advanced Institute of Science and Technology (2026).
[6] C. Filippone and K. A. Jordan, The Holos Reactor: A Distributable Power Generator with Transportable Subcritical Power Modules, Holos Generators.
[7] N. Stauff, C. Lee, P. Shriwise, Y. Miao, R. Hu, P. Vegendla, and T. Fei, Neutronic Design and Analysis of the Holos-Quad Concept: Progress of Holos ARPA-E Project from ANL Design Team, ANL/NSE-19/8, Argonne National Laboratory (2019).
[8] International Organization for Standardization, ISO 668:2020, Series 1 Freight Containers - Classification, Dimensions and Ratings (2020).
[9] U.S. Nuclear Regulatory Commission, Shielding Evaluation, Standard Review Plan for Transportation Packages for Radioactive Material, NUREG-2216, Chapter 5 (2020).
[10] Packaging and Transportation of Radioactive Material, 10 C.F.R. § 71.47.
[11] P. K. Romano and B. Forget, “The OpenMC Monte Carlo particle transport code,” Annals of Nuclear Energy, Vol. 51, pp. 274-281 (2013).
[12] International Commission on Radiological Protection, Conversion Coefficients for Radiological Protection Quantities for External Radiation Exposures, ICRP Publication 116, Ann. ICRP 40(2-5) (2010).